

New Large Signal Model of AlGaAs P-HEMT and GaAs MESFET Under Optical Illumination

J.M. Zamanillo, C. Navarro, C. Pérez-Vega, J.A. García, A. Mediavilla and A. Tazón

University of Cantabria - Communications Engineering Department (DICOM)

Av. de los Castros s/n. 39005, Santander, Spain. E-mail: jose.zamanillo@unican.es

As an extension of previous works in the optical-microwave interaction field, this paper shows the results of the research on large signal dynamic behaviour (Pulsed I/V curves) of AlGaAs P-HEMT (pseudomorphic high electron mobility transistor) devices, in the overall I/V plane, when the incident optical input power is changed. A complete bias and optical power dependence of the large signal model for a P-HEMT, is determined from experimental scattering parameters, DC and pulsed measurements. All derivatives of the model shown here are continuous for a realistic description of circuit distortion and intermodulation. The model is also valid for GaAs MESFET. Experimental results show very good agreement with theoretical analysis.

INTRODUCTION

The increasing use of microwave frequencies in communication systems, coupled with the ability to integrate microwave and optical components into a single wafer, usually denominated OMMIC (Optical Microwave Monolithic Integrated Circuit), have stimulated the interest in the development of microwave opto-electronic systems. GaAs MESFET devices are one of the most commonly active devices used in microwave circuit design and, many authors have developed accurate MESFET models including the optical effects. As far as we know, there is not an AlGaAs P-HEMT model that takes into account these effects, and this is the main reason because our group have taken interest on the development of the new electro-optical HEMT model reported in this paper. Furthermore, this model is valid for GaAs MESFET with no changes. A complete non-linear device model must take into account the different phenomena involved in the non-linear behaviour of the transistor. The large signal behaviour is governed by the dynamic pulsed I/V characteristics, which depend on the quiescent bias point. The results of the study presented here give a complete model of the optical large signal behaviour of HEMT devices, along with the knowledge of the optical laws for the most dependent parameters, including the non linear current sources I_{ds} and I_{gs} , and the capacitances C_{gs} and C_{ds} .

It is well known that when an AlGaAs HEMT is illuminated by a laser at fixed wavelength, absorption effects take place at the gate-drain and gate-source inter-electrode spaces, and free carrier photo-excitation is induced at the active area level. In fact, AlGaAs P-HEMTs, as GaAs MESFETs, exhibit both photoconductive and photovoltaic effects. This means that the static DC curves, as well as the small signal equivalent circuit parameters, change when optical energy is absorbed by the device..

OPTICAL LARGE SIGNAL DYNAMIC PROPERTIES

Our group (2-4) has shown the importance of non-linear characterisation of transistors from pulsed measurements. DC curves allow the knowledge of the DC and temperature behaviour of the quiescent operating points in RF operation, and the pulsed measurements take into account the transistor self-heating that change the internal parameters such as electron mobility, ionisation breakdown and Schottky barrier characteristics, even though low frequency dispersion, mainly on the transconductance and output conductance associated with deep level traps and surface state, greatly affects the dynamic behaviour of the transistor. The equivalent circuit used, show in Fig. 1(a), is a rather general one and is applicable to AlGaAs PHEMT and GaAs MESFET devices. This work uses the MESFET equivalent circuit reported by us (1) for illuminated devices, with several modifications on the expression of the I_{ds} current source, as well as for the non linear I_{gs} source in order to take into account the optical dependence. The equation for the dynamic current I_{ds} , is modified according to Allemand and Bonnaire (5) in order to guarantee the continuity of the derivatives. Therefore, the I_{ds} equation is given by:

$$I_{ds} = I_{dss} \cdot \left\{ \frac{a \cdot (V_{gi} - V_t) + \log \left\{ 2 \cdot \cosh \left[a \cdot (V_{gi} - V_t) \right] \right\}}{2 \cdot b \cdot |V_t|} \right\}^{(E + K_s \cdot V_{gi})} \cdot (1 + S_s \cdot V_{di}) \cdot \tanh \left(\frac{S_l \cdot V_{di}}{1 - K_g \cdot V_{gi}} \right) + C \cdot V_{di} \quad (1)$$

with: $V_t = V_{t0} + \gamma \cdot V_{di}$

where V_{gi} and V_{di} are the internal instantaneous voltages, γ , E , S_l , K_g , a and b are constants, and I_{dss} , V_{t0} , S_s , K_e , and C are the optical power (PL) dependent parameters in order to fit the pulsed I/V dynamic

behaviour with the optical power applied to the device, as follows:

$$C = C_1 \cdot PL \quad (2)$$

$$Ke = Ke_0 + Ke_1 \cdot PL \quad (3)$$

$$Ss = Ss_0 + Ss_1 \cdot PL^{Ss_2} \quad (4)$$

$$Vt0 = Vt0_0 + Vt0_1 \cdot PL^{Vt0_2} + Vt0_3 \cdot PL \quad (5)$$

$$Idss = Idss_0 + Idss_1 \cdot PL^{Idss_2} + Idss_3 \cdot PL \quad (6)$$

where these new set of parameters, C_1 , Ke_0, Ke_1 , Ss_0 , Ss_1 , Ss_2 , $Vt0_0, Vt0_1$, $Vt0_2, Vt0_3$, $Idss_0$, $Idss_1$, $Idss_2$ and $Idss_3$ are functions of the quiescent bias point. The new expression is also valid for GaAs MESFET devices, making the parameters $a=b$ and $C=0$ only, so this new approach is valid for MESFET and HEMT devices. The non-linear capacitances C_{gd} and C_{gs} are modelled based on the model of Scheimberg and Chrisolm (6) according to that reported in (4), giving by the following expressions:

$$C_{gd} = C_{gd0} \cdot \left[1 + C_f \tanh \left(S_g [V_{GD} - D_C \tanh(D_k V_{GS})] \right) \right] + m \cdot PL \quad (7)$$

$$C_{gs} = C_{gs0} \cdot \left[1 + C_f \tanh \left(S_g [V_{GS} - D_C \tanh(D_k V_{GD})] \right) \right] \quad (8)$$

Figure 2 shows the measured and modelised static and dynamic I/V curves for a D02AH process $4 \times 30 \mu\text{m}$ (4 finger by 30 microns gate-width) Philips AlGaAs P-HEMT device. Both curves, static and dynamic, also show the excellent fit of the model reported in this paper, and they are measured under 10mW of laser illumination power. It can be observed, as could be expected from physical considerations, that there is noticeable change in the drain slopes, along with the normal increment of the drain current. A new expression to describe the non-linear current source I_{gs} , has been used. This new equation is the sum of two terms: one is the typical Schottky expression valid for the non-illuminated device and the second takes into account the current induced by the optical power:

$$I_{gs} = I_{gs} \Big|_{PL=0} + I_{gsHL} = I_{gs0} \left(e^{I_{gs1} V_{gi}} - 1 \right) + g_1 \cdot e^{g_2 \cdot V_{gi}} \cdot \left(1 + \frac{g_3 \cdot e^{g_4 \cdot V_{gi}}}{1 + g_5 \cdot e^{V_{di}}} \right) \quad (9)$$

where g_2 and g_3 only depend of the device size (gate length) and do not vary with the optical power, but g_1 , g_4 y g_5 show polynomial and exponential variations with the applied optical (PL) in accordance with the following expressions.

$$g_1 = g_{11} \cdot PL + g_{12} \cdot PL^2 + g_{13} \cdot PL^3 \quad (10)$$

$$g_4 = g_{40} + g_{41} \cdot PL^{g_{42}} \quad (11)$$

$$g_5 = g_{50} + g_{51} \cdot PL^{g_{52}} \quad (12)$$

Furthermore, we assumed that the I_{gd} current source follows a linear expression.

$$I_{gd} = g_{gd} \cdot V_{gdo} \quad (13)$$

where g_{gd} is the output conductance extracted from the small-signal model. The output capacitance C_{ds} is assumed linear. This expression concludes the explanation of all non-linearities of this new large signal model.

Parasitic elements are extracted from multibias scattering measurements using conventional techniques reported by Dambrine et al. (7), under the assumption that they do not vary with bias point and optical power applied (PL). Figures 3 and 4 show a comparison between modelled and measured scattering parameters for a $PL=2\text{mW}$. The simulation has been performed using the model presented in this paper and the ADS simulator from Agilent Technologies.

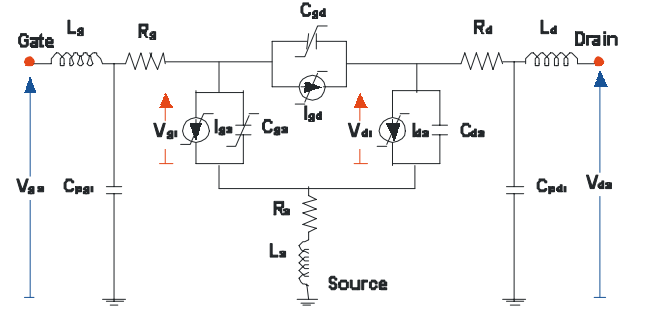


Figure 1: Large Signal equivalent circuit of AlGaAs P-HEMT and GaAs MESFET under Optical Illumination.

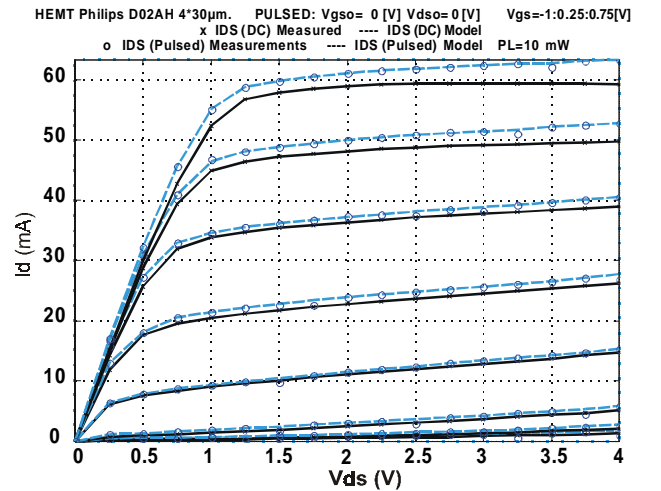


Figure 2: Comparison between measured and modelled static and dynamic I-V curves for a $4 \times 30 \mu\text{m}$ AlGaAs PHEMT

References

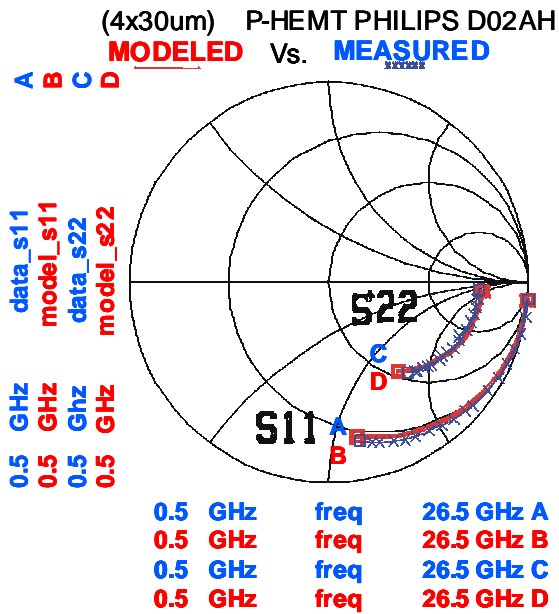


Figure 3: S11 and S22 comparison using our model and measurements of the scattering parameters at $V_{gs}=0.25$, $V_{ds}=2V$ and $PL=2$ mW

Figure 4: S21 and S12 comparison using our model and measurements of the scattering parameters at $(V_{gs}, V_{ds})=(0.25, 2.00)$ $PL=2$ mW

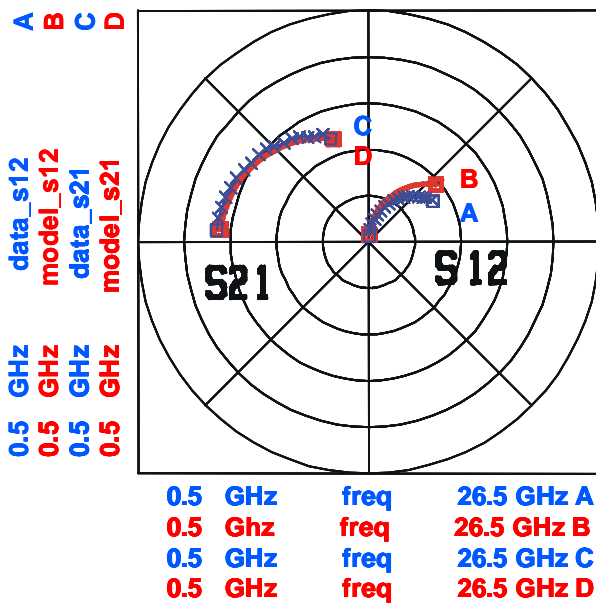


Figure 4: S21 and S12 comparison using our model and measurements of the scattering parameters at $V_{gs}=0.25$, $V_{ds}=2V$ and $PL=2$ mW.

The model is also capable of predicting the figures of merit of the transistor. As an example, a comparison between the computed values of the Rollet's factor computed from measurements and given by the model is shown in figure 5(a) for the 6 by 30 μ m PHILIPS P-HEMT and two different optical powers (0 and 7.5 mW) applied.

Figure 5(b) shows a comparison between the maximum stable gain and the maximum available gain computed by the model and measurements for 2mW of optical power applied to the same device

CONCLUSIONS

An exhaustive investigation on the dynamic properties of AlGaAs PHEMT devices under optical illumination has been performed. The main dependencies and the way of integrating this behaviour into any classical analytical equation for the drain and gate currents has been shown. The model presented here is also valid for GaAs MESFET devices. Numerical simulations show good experimental agreement. This electro-optical model provides much greater accuracy and flexibility than previous models in both linear and saturation regions as a function of V_{gs} , V_{gd} and PL . The capacitor fitting parameters are not involved in the simulation of any other device non-linearities, thus allowing independent simulation of static and dynamic behaviour and high execution speed. This allows the new expressions to be easily used in designs containing electro-optical devices such as optical switching as well as oscillators with optical tuning or optical injection tuning (8) with a higher degree of confidence.

ACKNOWLEDGEMENT

This work has been developed within the framework of a Spanish project of the Comisión Interministerial de Ciencia y Tecnología (TIC2000-0401-P4-09).

REFERENCES

- (1) J.M. Zamanillo, C. Navarro, C. Pérez-Vega, A. Mediavilla, and A. Tazón *Large Signal Model Predicts Dynamic Behavior of GaAs MESFET Under Optical Illumination*. Microwave and Optical Technology Letters. Vol. 29 No.1, pp 25-31. April 5 2001.
- (2) T. Fernández, Y. Newport, J. M. Zamanillo, A. Mediavilla, A. Tazón. *High Speed Automated Pulsed I/V Measurement System*". 23rd EuMC, Madrid, Sep. 1993, pp. 494-496.
- (3) J.M. Zamanillo, C. Navarro, J. Sáiz-Ipiña, C. Pérez-Vega and A. Mediavilla. "New Large Signal Electrical Model of GaAs MESFET Under Optical Illumination". European Microwave Week, GaAs 2001 proceedings, pp.167-170, London, Sept-2001.
- (4) C. Navarro, J.M. Zamanillo, A. Mediavilla, A. Tazón and J.L. García *New Optical Capacitance Model for GaAs MESFETs*. Microwave and Optical Technology Letters. Vol. 26 No.1, July 5 2000, pp 16-21.
- (5) E. Allemand and Y. Bonnaire. *Nonlinearities of the GaAs Submicrometer FET: New Mode of Characterization and Modelization*, 18th European Microwave Conference Proceedings, Stockholm, Set.1988, pp.243-248.
- (6) Norman Scheinberg and Ellis Chisholm. *A Capacitance Model for GaAs MESFET*. IEEE Journal of Solid-State Circuits, Vol 26, No 10, Oct 1991 pp. 1467-1470.

(7) G. Dambrine, A. Cappy, F. Heliodore, and E. Playez, *A New Method of determining the FET small-signal equivalent circuit*, IEEE Trans. MTT, Vol 36, July 1988, pp. 1151-1159.

(8) A.J. Seeds, A.A.A. Salles. *Optical Control of Microwave Semiconductor Devices*. IEEE Trans. MTT, Vol 38, No 5, pp. 577-585, May 1990

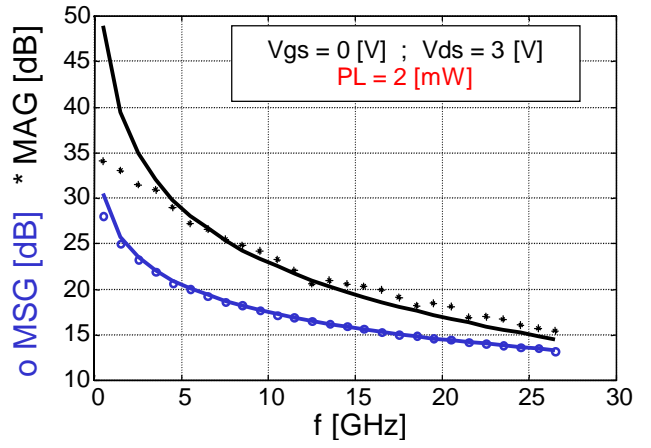
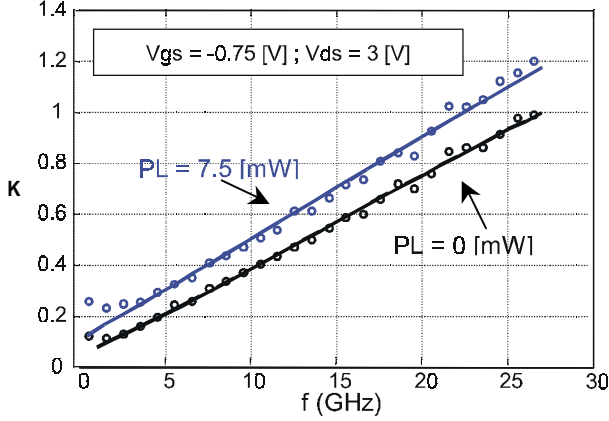


Figure 5(a): Rollet's factor comparison using the model presented here and computed from measurements for optical powers of 0mW and 7.5mW.

Figure 5(b): Maximum Stable Gain and Maximum Stable Gain comparison using the model presented here and computed from measurements for optical power of 2mW.

Table 1

Parameters of the complete model

Cgs Parameters			
$C_0 = 0.0326$	$S_g = 0.7818$	$D_k = 0.9599$	
$C_1 = -0.0046$	$C_2 = -0.0013$	$C_3 = 4.2904$	$C_4 = 1.1795$
$C_{f0} = 1.4136$	$C_{f1} = 9.4644 \cdot 10^9$	$C_{f2} = 1.5826 \cdot 10^7$	$C_{f3} = 0.5453$
$D_{c0} = 1.0645$	$D_{c1} = 0.0123$		
Cgd Parameters			
$C_{gd0} = 0.0145$	$m = -0.3167 \cdot 10^{-3}$		
Parameters of Ids			
$\gamma = -0.0689$	$E = 1.7999$	$SI = 3.8200$	$Kg = -1.3173$
$a = 15.8857$	$b = 4.5598$	$C_1 = 0.0310$	
$Ke_0 = -0.2988$	$Ke_1 = 0.0011$		
$Ss_0 = 0.1241$	$Ss_1 = -0.0209$	$Ss_2 = 0.2299$	
$Vt_0 = -0.4782$	$Vt_1 = -0.0192$	$Vt_2 = 0.0271$	$Vt_3 = -0.0028$
$Idss_0 = 1.9238$	$Idss_1 = 0.1518$	$Idss_2 = 0.1785$	$Idss_3 = 0.0055$
Parameters of Igs			
$Igs_0 = 1.0504 \cdot 10^{-21}$	$Igs_1 = 65.5714$	$g_2 = -1.0863$	$g_3 = 0.4025$
$g_{11} = -2.45 \cdot 10^{-3}$	$g_{12} = -5.84 \cdot 10^{-4}$	$g_{13} = 4.42 \cdot 10^{-5}$	
$g_{40} = 0.1387$	$g_{41} = -1.8603$	$g_{42} = -0.5945$	
$g_{50} = 0.5554$	$g_{51} = 10.1393$	$g_{50} = -3.8497$	
Parasitic Elements			
$R_g = 6.60 \Omega$	$R_d = 6.10 \Omega$	$R_s = 7.10 \Omega$	$C_{pgi} = 10.20 \text{ fF}$
$L_g = 0.035 \text{ nH}$	$L_d = 0.011 \text{ nH}$	$L_s = 0 \text{ nH}$	$C_{pdi} = 9.00 \text{ fF}$